Bayes-Adaptive Simulation-based Search with Value Function Approximation

Arthur Guez[*,1,2] **Nicolas Heess**[2] **David Silver**[2] **Peter Dayan**[1]

[*]aguez@google.com [1]Gatsby Unit, UCL [2]Google DeepMind

Abstract

Bayes-adaptive planning offers a principled solution to the exploration-exploitation trade-off under model uncertainty. It finds the optimal policy in belief space, which explicitly accounts for the expected effect on future rewards of reductions in uncertainty. However, the Bayes-adaptive solution is typically intractable in domains with large or continuous state spaces. We present a tractable method for approximating the Bayes-adaptive solution by combining simulation-based search with a novel value function approximation technique that generalises appropriately over belief space. Our method outperforms prior approaches in both discrete bandit tasks and simple continuous navigation and control tasks.

1 Introduction

A fundamental problem in sequential decision making is controlling an agent when the environmental dynamics are only partially known. In such circumstances, probabilistic models of the environment are used to capture the uncertainty of current knowledge given past data; they thus imply how exploring the environment can be expected to lead to new, exploitable, information.

In the context of Bayesian model-based reinforcement learning (RL), Bayes-adaptive (BA) planning [8] solves the resulting exploration-exploitation trade-off by directly optimizing future expected discounted return in the joint space of states and beliefs about the environment (or, equivalently, interaction histories). Performing such optimization even approximately is computationally highly challenging; however, recent work has demonstrated that online planning by sample-based forward-search can be effective [22, 1, 12]. These algorithms estimate the value of future interactions by simulating trajectories while growing a search tree, taking model uncertainty into account. However, one major limitation of Monte Carlo search algorithms in general is that, naïvely applied, they fail to generalize values between related states. In the BA case, a separate value is stored for each distinct path of possible interactions. Thus, the algorithms fail not only to generalize values between related paths, but also to reflect the fact that different histories can correspond to the same belief about the environment. As a result, the number of required simulations grows exponentially with search depth. Worse yet, except in very restricted scenarios, the lack of generalization renders MC search algorithms effectively inapplicable to BAMDPs with continuous state or action spaces.

In this paper, we propose a class of efficient simulation-based algorithms for Bayes-adaptive model-based RL which use function approximation to estimate the value of interaction histories during search. This enables *generalization* between different beliefs, states, and actions during planning, and therefore also works for continuous state spaces. To our knowledge this is the first broadly applicable MC search algorithm for continuous BAMDPs.

Our algorithm builds on the success of a recent tree-based algorithm for discrete BAMDPs (BAMCP, [12]) and exploits value function approximation for generalization across interaction histories, as has been proposed for simulation-based search in MDPs [19]. As a crucial step towards this end we develop a suitable parametric form for the value function estimates that can generalize appropriately

across histories, using the importance sampling weights of posterior samples to compress histories into a finite-dimensional feature vector. As in BAMCP we take advantage of *root sampling* [18, 12] to avoid expensive belief updates at every step of simulation, making the algorithm practical for a broad range of priors over environment dynamics. We also provide an interpretation of root sampling as an auxiliary variable sampling method. This leads to a new proof of its validity in general simulation-based settings, including BAMDPs with continuous state and action spaces, and a large class of algorithms that includes MC and TD upates.

Empirically, we show that our approach requires considerably fewer simulations to find good policies than BAMCP in a (discrete) bandit task and two continuous control tasks with a Gaussian process prior over the dynamics [5, 6]. In the well-known pendulum swing-up task, our algorithm learns how to balance after just a few seconds of interaction. Below, we first briefly review the Bayesian formulation of optimal decision making under model uncertainty (section 2; please see [8] for additional details). We then explain our algorithm (section 3) and present empirical evaluations in section 4. We conclude with a discussion, including related work (sections 5 and 6).

2 Background

A Markov Decision Processes (MDP) is described as a tuple $M = \langle S, A, \mathcal{P}, \mathcal{R}, \gamma \rangle$ with S the set of states (which may be infinite), A the *discrete* set of actions, $\mathcal{P} : S \times A \times S \to \mathbb{R}$ the state transition probability kernel, $\mathcal{R} : S \times A \to \mathbb{R}$ the reward function, and $\gamma < 1$ the discount factor. The agent starts with a prior $P(\mathcal{P})$ over the dynamics, and maintains a posterior distribution $b_t(\mathcal{P}) = P(\mathcal{P}\,|h_t) \propto P(h_t|\,\mathcal{P})P(\mathcal{P})$, where h_t denotes the history of states, actions, and rewards up to time t.

The uncertainty about the dynamics of the model can be transformed into certainty about the current state inside an augmented state space $S^+ = \mathcal{H} \times S$, where $\mathcal{H}$ is the set of possible histories (the current state also being the suffix of the current history). The dynamics and rewards associated with this augmented state space are described by

$$\mathcal{P}^+(h, s, a, has', s') = \int_{\mathcal{P}} \mathcal{P}(s, a, s')P(\mathcal{P}|h)\,\mathrm{d}\mathcal{P}, \quad \mathcal{R}^+(h, s, a) = R(s, a). \tag{1}$$

Together, the 5-tuple $M^+ = \langle S^+, A, \mathcal{P}^+, \mathcal{R}^+, \gamma \rangle$ forms the Bayes-Adaptive MDP (BAMDP) for the MDP problem M. Since the dynamics of the BAMDP are known, it can in principle be solved to obtain the optimal value function associated with each action:

$$Q^*(h_t, s_t, a) = \max_{\tilde{\pi}} \mathbb{E}_{\tilde{\pi}} \left[\sum_{t'=t}^{\infty} \gamma^{t'-t} r_{t'} | a_t = a \right]; \quad \tilde{\pi}^*(h_t, s_t) = \operatorname*{argmax}_a Q^*(h_t, s_t, a), \tag{2}$$

where $\tilde{\pi} : S^+ \times A \to [0, 1]$ is a policy over the augmented state space, from which the optimal action for each belief-state $\tilde{\pi}^*(h_t, s_t)$ can readily be derived. Optimal actions in the BAMDP are executed greedily in the real MDP M, and constitute the best course of action (i.e., integrating exploration and exploitation) for a Bayesian agent with respect to its prior belief over $\mathcal{P}$.

3 Bayes-Adaptive simulation-based search

Our simulation-based search algorithm for the Bayes-adaptive setup combines efficient MC search via root-sampling with value function approximation. We first explain its underlying idea, assuming a suitable function approximator exists, and provide a novel proof justifying the use of root sampling that also applies in continuous state-action BAMDPs. Finally, we explain how to model Q-values as a function of interaction histories.

3.1 Algorithm

As in other forward-search planning algorithms for Bayesian model-based RL [22, 17, 1, 12], at each step t, which is associated with the current history h_t (or belief) and state s_t, we plan online to find $\tilde{\pi}^*(h_t, s_t)$ by constructing an action-value function $Q(h, s, a)$. Such methods use simulation to build a search *tree* of belief states, each of whose nodes corresponds to a single (future) history, and estimate optimal values for these nodes. However, existing algorithms only update the nodes that are directly traversed in each simulation. This is inefficient, as it fails to generalize across multiple histories corresponding either to *exactly* the same, or similar, beliefs. Instead, each such history must be traversed and updated separately.

Here, we use a more general simulation-based search that relies on function approximation, rather than a tree, to represent the values for possible simulated histories and states. This approach was originally suggested in the context of planning in large MDPs[19]; we extend it to the case of Bayes-Adaptive planning. The Q-value of a particular history, state, and action is represented as $Q(h, s, a; \mathbf{w})$, where $\mathbf{w}$ is a vector of learnable parameters. Fixed-length simulations are run from the current belief-state h_t, s_t, and the parameter $\mathbf{w}$ is updated online, during search, based on experience accumulated along these trajectories, using an incremental RL control algorithm (e.g., Monte-Carlo control, Q-learning). If the parametric form and features induce generalization between histories, then each forward simulation can affect the values of histories that are not directly experienced. This can considerably speed up planning, and enables continuous-state problems to be tackled. Note that a search tree would be a special case of the function approximation approach when the representation of states and histories is tabular.

In the context of Bayes-Adaptive planning, simulation-based search works by simulating a future trajectory $h_{t+T} = s_t a_t r_t s_{t+1} \dots a_{t+T-1} r_{t+T-1} s_{t+T}$ of T transitions (the planning horizon) starting from the current belief-state h_t, s_t. Actions are selected by following a fixed policy $\tilde{\pi}$, which is itself a function of the history, $a \sim \tilde{\pi}(h, \cdot)$. State transitions can be sampled according to the BAMDP dynamics, $s_{t'} \sim \mathcal{P}^+(h_{t'-1}, s_{t'-1}, a_{t'}, h_{t'-1}a_{t'}\cdot, \cdot)$. However, this can be computationally expensive since belief updates must be applied at every step of the simulation. As an alternative, we use root sampling [18], which only samples the dynamics $\mathcal{P}^k \sim P(\mathcal{P}\,|h_t)$ once at the root for each simulation k and then samples transitions according to $s_{t'} \sim \mathcal{P}^k(s_{t'-1}, a_{t'-1}, \cdot)$; we provide justification for this approach in Section 3.2.[1] After the trajectory h_T has been simulated on a step, the Q-value is modified by updating $\mathbf{w}$ based on the data in h_{t+T}. Any incremental algorithm could be used, including SARSA, Q-learning, or gradient TD [20]; we use a simple scheme to minimize an appropriately weighted squared loss $\mathbb{E}[(Q(h_{t'}, s_{t'}, a_{t'}; \mathbf{w}) - R_{t'})^2]$:

Algorithm 1: Bayes-Adaptive simulation-based search with root sampling

procedure `Search(` h_t, s_t `)`
  repeat
    $\mathcal{P} \sim P(\mathcal{P}\,|h_t)$
    `Simulate(`$h_t, s_t, \mathcal{P}, 0$`)`
  until `Timeout()`
  return $\text{argmax}_a\ Q(h_t, s_t, a; \mathbf{w})$
end procedure
procedure `Simulate(` $h, s, \mathcal{P}, t$ `)`
  if $t > T$ **then return** 0
  $a \leftarrow \tilde{\pi}_{\epsilon-\text{greedy}}(Q(h, s, \cdot; \mathbf{w}))$
  $s' \sim \mathcal{P}(s, a, \cdot), r \leftarrow \mathcal{R}(s, a)$
  $R \leftarrow r + \gamma$ `Simulate(`$has', s', \mathcal{P}, t{+}1$`)`
  $\mathbf{w} \leftarrow \mathbf{w} - \alpha\,(Q(h, s, a; \mathbf{w}) - R)\,\nabla_{\mathbf{w}} Q(h, s, a; \mathbf{w})$
  return R
end procedure

$$|\Delta\,\mathbf{w}\,| = \alpha\ (Q(h_{t'}, s_{t'}, a_{t'}; \mathbf{w}) - R_{t'})\,\nabla_{\mathbf{w}} Q(h_{t'}, s_{t'}, a_{t'}; \mathbf{w}), \tag{3}$$

where α is the learning rate and $R_{t'}$ denotes the discounted return obtained from history $h_{t'}$.[2] Algorithm 1 provides pseudo-code for this scheme; here we suggest using as the fixed policy for a simulation the $\epsilon-$greedy $\tilde{\pi}_{\epsilon-\text{greedy}}$ based on some given Q value. Other policies could be considered (e.g., the UCT policy for search trees), but are not the main focus of this paper.

3.2 Analysis

In order to exploit general results on the convergence of classical RL algorithms for our simulation-based search, it is necessary to show that starting from the current history, root sampling produces the appropriate distribution of rollouts. For the purpose of this section, a simulation-based search algorithm includes Algorithm 1 (with Monte-Carlo backups) but also incremental variants, as discussed above, or BAMCP.

Let $\mathcal{D}_t^{\tilde{\pi}}$ be the *rollout distribution* function of forward-simulations that explicitly updates the belief at each step (i.e., using $\mathcal{P}^+$): $\mathcal{D}_t^{\tilde{\pi}}(h_{t+T})$ is the probability density that history h_{t+T} is generated when running that simulation from h_t, s_t, with T the horizon of the simulation, and $\tilde{\pi}$ an arbitrary history policy. Similarly define the quantity $\tilde{\mathcal{D}}_t^{\tilde{\pi}}(h_{t+T})$ as the probability density that history h_{t+T} is generated when running forward-simulations *with root sampling*, as in Algorithm 1. The following lemma shows that these two rollout distributions are the same.

[1] For comparison, a version of the algorithm without root sampling is listed in the supplementary material.

[2] The loss is weighted according to the distr. of belief-states visited from the current state by executing $\tilde{\pi}$.

Lemma 1. $\mathcal{D}_t^{\tilde{\pi}}(h_{t+T}) = \tilde{\mathcal{D}}_t^{\tilde{\pi}}(h_{t+T})$ *for all policies* $\tilde{\pi} : \mathcal{H} \times A \to [0,1]$ *and for all* $h_{t+T} \in \mathcal{H}$ *of length* $t+T$.

Proof. A similar result has been obtained for discrete state-action spaces as Lemma 1 in [12] using an induction step on the history length. Here we provide a more intuitive interpretation of root sampling as an auxiliary variable sampling scheme which also applies directly to continuous spaces. We show the equivalence by rewriting the distribution of rollouts. The usual way of sampling histories in simulation-based search, with belief updates, is justified by factoring the density as follows:

$$
\begin{aligned}
p(h_{t+T}|h_t, \tilde{\pi}) &= p(a_t s_{t+1} a_{t+1} s_{t+2} \dots s_{t+T}|h_t, \tilde{\pi}) && (4)\\
&= p(a_t|h_t, \tilde{\pi}) p(s_{t+1}|h_t, \tilde{\pi}, a_t) p(a_{t+1}|h_{t+1}, \tilde{\pi}) \dots p(s_{t+T}|h_{t+T-1}, a_{t+T}, \tilde{\pi}) && (5)\\
&= \prod_{t \le t' < t+T} \tilde{\pi}(h_{t'}, a_{t'}) \prod_{t < t' \le t+T} p(s_{t'}|h_{t'-1}, \tilde{\pi}, a_{t'-1}) && (6)\\
&= \prod_{t \le t' < t+T} \tilde{\pi}(h_{t'}, a_{t'}) \prod_{t < t' \le t+T} \int_{\mathcal{P}} P(\mathcal{P}\,|h_{t'-1})\, \mathcal{P}(s_{t'-1}, a_{t'-1}, s_{t'})\, \mathrm{d}\mathcal{P}, && (7)
\end{aligned}
$$

which makes clear how each simulation step involves a belief update in order to compute (or sample) the integrals. Instead, one may write the history density as the marginalization of the joint over history and the dynamics $\mathcal{P}$, and then notice that an history is generated in a Markovian way *if conditioned on the dynamics*:

$$
\begin{aligned}
p(h_{t+T}|h_t, \tilde{\pi}) &= \int_{\mathcal{P}} p(h_{t+T}|\,\mathcal{P}, h_t, \tilde{\pi}) p(\mathcal{P}\,|h_t, \tilde{\pi})\, \mathrm{d}\mathcal{P} = \int_{\mathcal{P}} p(h_{t+T}|\,\mathcal{P}, \tilde{\pi}) p(\mathcal{P}\,|h_t)\, \mathrm{d}\mathcal{P} && (8)\\
&= \int_{\mathcal{P}} \prod_{t \le t' < t+T} \tilde{\pi}(h_{t'}, a_{t'}) \prod_{t < t' \le t+T} \mathcal{P}(s_{t'-1}, a_{t'-1}, s_{t'})\;\; p(\mathcal{P}\,|h_t)\, \mathrm{d}\mathcal{P}, && (9)
\end{aligned}
$$

where eq. (9) makes use of the Markov assumption in the MDP. This makes clear the validity of sampling only from $p(\mathcal{P}\,|h_t)$, as in root sampling. From these derivations, it is immediately clear that $\mathcal{D}_t^{\tilde{\pi}}(h_{t+T}) = \tilde{\mathcal{D}}_t^{\tilde{\pi}}(h_{t+T})$. □

The result in Lemma 1 does not depend on the way we update the value Q, or on its representation, since the policy is fixed for a given simulation.[3] Furthermore, the result guarantees that simulation-based searches will be identical in distribution with and without root sampling. Thus, we have:

Corollary 1. *Define a Bayes-adaptive simulation-based planning algorithm as a procedure that repeatedly samples future trajectories* $h_{t+T} \sim \mathcal{D}_t^{\tilde{\pi}}$ *from the current history* h_t *(simulation phase), and updates the Q value after each simulation based on the experience* h_{t+T} *(special cases are Algorithm 1 and* BAMCP*). Then such a simulation-based algorithm has the same distribution of parameter updates with or without root sampling. This also implies that the two variants share the same fixed-points, since the updates match in distribution.*

For example, for a discrete environment we can choose a tabular representation of the value function in history space. Applying the MC updates in eq. (3) results in a MC control algorithm applied to the sub-BAMDP from the root state. This is exactly the (BA version of the) MC tree search algorithm [12]. The same principle can also be applied to MC control with function approximation with convergence results under appropriate conditions [2]. Finally, more general updates such as gradient Q-learning could be applied with corresponding convergence guarantees [14].

3.3 History Features and Parametric Form for the Q-value

The quality of a history policy obtained using simulation-based search with a parametric representation $Q(h, s, a; \mathbf{w})$ crucially depends on the features associated with the arguments of Q, i.e., the history, state and action. These features should arrange for histories that lead to the same, or similar, beliefs have the same, or similar, representations, to enable appropriate generalization. This is challenging since beliefs can be infinite-dimensional objects with non-compact sufficient statistics that are therefore hard to express or manipulate. Learning good representations from histories is also tough, for instance because of hidden symmetries (e.g., the irrelevance of the order of the experience tuples that lead to a particular belief).

[3] Note that, in Algorithm 1, Q is only updated *after* the simulation is complete.

We propose a parametric representation of the belief at a particular planning step based on *sampling*. That is, we draw a set of M independent MDP samples or particles $U = \{\mathcal{P}_1, \mathcal{P}_2, \ldots, \mathcal{P}_M\}$ from the current belief $b_t = P(\mathcal{P}\,|h_t)$, and associate each with a weight $z^U_m(h)$, such that the vector $z^U(h)$ is a finite-dimensional approximate representation of the belief based on the set U. We will also refer to z^U as a function $z^U : \mathcal{H} \to \mathbb{R}^M$ that maps histories to a *feature vector*.

There are various ways one could design the z^U function. It is computationally convenient to compute $z^U(h)$ recursively as importance weights, just as in a sequential importance sampling particle filter [11]; this only assumes we have access to the likelihood of the observations (i.e., state transitions). In other words, the weights are initialized as $z^U_m(h_t) = \frac{1}{M}\ \forall m$ and are then updated recursively using the likelihood of the dynamics model for that particle of observations as $z^U_m(has') \propto z^U_m(h)P(s'|a,s,\mathcal{P}_m) = z^U_m(h)\,\mathcal{P}_m(s,a,s')$.

One advantage of this definition is that it enforces a correspondence between the history and belief representations in the finite-dimensional space, in the sense that $z_U(h') = z_U(h)$ if belief$(h) =$ belief(h'). That is, we can work in history space *during planning*, alleviating the need for complete belief updates, but via a finite and well-behaved representation of the actual belief — since different histories corresponding to the same belief are mapped to the same representation.

This feature vector can be combined with any function approximator. In our experiments, we combine it with features of the current state and action, $\phi(s,a)$, in a simple bilinear form:

$$Q(h,s,a;\mathbf{W}) = z_U(h)^T\,\mathbf{W}\,\phi(s,a), \tag{10}$$

where $\mathbf{W}$ is the matrix of learnable parameters adjusted during the search (eq. 3). Here $\phi(s,a)$ is a domain-dependent state-action feature vector as is standard in fully observable settings with function approximation. Special cases include tabular representations or forms of tile coding. We discuss the relation of this parametric form to the true value function in the Supp. material.

In the next section, we investigate empirically in three varied domains the combination of this parametric form, simulation-based search and Monte-Carlo backups, collectively known as BAFA (for *B*ayes *A*daptive planning with *F*unction *A*pproximation).

4 Experimental results

The discrete *Bernoulli bandit* domain (section 4.1) demonstrates dramatic efficiency gains due to generalization with convergence to a near Bayes-optimal solution. The *navigation task* (section 4.2) and the *pendulum* (section 4.3) demonstrate the ability of BAFA to handle non-trivial planning horizons for large BAMDPs with continuous states. We provide comparisons to a state of the art BA tree-search algorithm (BAMCP, [12]), choosing a suitable discretization of the state space for the continuous problems. For the pendulum we also compare to two Bayesian, but not Bayes adaptive, approaches.

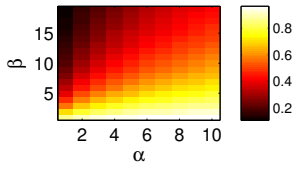

(a) $m_{\alpha,\beta}$

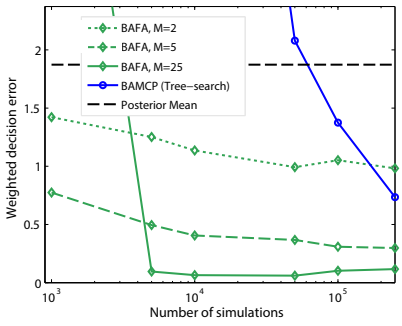

(b)

Figure 1: a) The weights $m_{\alpha,\beta}$ b) Averaged (weighted) decision errors for the different methods as a function of the number of simulations.

4.1 Bernoulli Bandit

Bandits have simple dynamics, yet they are still challenging for a generic Bayes-Adaptive planner. Importantly, ground truth is sometimes available [10], so we can evaluate how far the approximations are from Bayes-optimality.

We consider a 2-armed Bernoulli bandit problem. We oppose an uncertain arm with prior success probability $p_1 \sim Beta(\alpha,\beta)$ against an arm with known success probability p_0. We consider the scenario $\gamma = 0.99, p_0 = 0.2$ for which the optimal decision, and the posterior mean decision frequently differ. Decision errors for different values of α,β do not have the same consequence, so we weight each scenario according to the difference between their associated Gittins indices. Define the weight as $m_{\alpha,\beta} = |g_{\alpha,\beta} - p_0|$ where $g_{\alpha,\beta}$ is the Gittins index for α,β; this is an upper-bound (up to a scaling factor) on the difference between the value of the arms. The weights are shown in Figure 1-a.

We compute the weighted errors over 20 runs for a particular method as $E_{\alpha,\beta} = m_{\alpha,\beta} \cdot P(\text{Wrong decision for } (\alpha,\beta))$, and report the sum of these terms across the range $1 \leq \alpha \leq 10$ and $1 \leq \beta \leq 19$ in Figure 1-b as a function of the number of simulations.

Though this is a discrete problem, these results show that the value function approximation approach, even with a limited number of particles (M) for the history features, learns considerably more quickly than BAMCP . This is because BAFA generalizes between similar beliefs.

4.2 Height map navigation

We next consider a 2-D navigation problem on an unknown continuous height map. The agent's state is (x, y, z, θ), it moves on a bounded region of the $(x, y) \in 8 \times 8m$ plane according to (known) noisy dynamics. The agent chooses between 5 different actions, the dynamics for (x, y) are $(x_{t+1}, y_{t+1}) = (x_t, y_t) + l(\cos(\theta_a), \sin(\theta_a)) + \boldsymbol{\epsilon}$, where θ_a corresponds to the action from this set $\theta_a \in \theta + \{-\frac{\pi}{3}, -\frac{\pi}{6}, 0, \frac{\pi}{6}, \frac{\pi}{3}\}$, $\boldsymbol{\epsilon}$ is small isotropic Gaussian noise ($\sigma = 0.05$), and $l = \frac{1}{3}$m is the step size. Within the bounded region, the reward function is the value of a latent height map $z = f(x, y)$ which is only observed at a single point by the agent. The height map is a draw from a Gaussian process (GP), $f \sim GP(0, \mathcal{K})$, using a multi-scale squared exponential kernel for the covariance matrix and zero mean. In order to test long-horizon planning, we downplay situations where the agents can simply follow the expected gradient locally to reach high reward regions by starting the agent on a small local maximum. To achieve this we simply condition the GP draw on a few pseudo-observations with small negative z around the agent and a small positive z at the starting position, which creates a small bump (on average). The domain is illustrated in Figure 2-a with an example map.

We compare BAMCP against BAFA on this domain, planning over 75 steps with a discount of 0.98. Since BAMCP works with discrete state, we uniformly discretize the height observations. For the state-features in BAFA, we use a regular tile coding of the space; an RBF network leads to similar results. We use a common set of a 100 ground truth maps drawn from the prior for each algorithm/setting, and we average the discounted return over 200 runs (2 runs/map) and report that result in Figure 2-b as a function of the planning horizon (T). This result illustrates the ability of BAFA to cope with non-trivial planning horizons in belief space. Despite the discretization, BAMCP is very efficient with short planning horizons, but has trouble optimizing the history policy with long horizons because of the huge tree induced by the discretization of the observations.

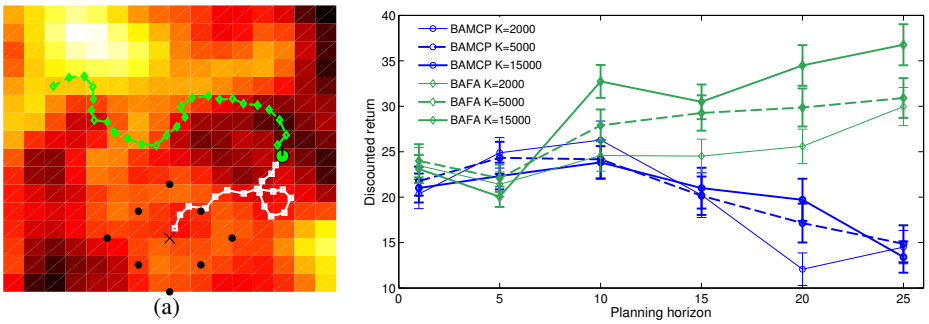

(a) (b)

Figure 2: (a) Example map showing with the height color-coded from white (negative reward z) to black (positive reward z). The black dots denote the location of the initial pseudo-observations used to obtain the ground truth map. The white squares show the past trajectory of the agent, starting at the cross and ending at the current position in green. The green trajectory is one particular forward simulation of BAFA from that position. (b) Averaged discounted return (higher is better) in the navigation domain for discretized BAMCP and BAFA as a function of the number of simulations (K), and as function of the planning horizon (x-axis).

4.3 Under-actuated Pendulum Swing-up

Finally, we consider the classic RL problem in which an agent must swing a pendulum from hanging vertically down to balancing vertically up, but given only limited torque. This requires the agent to build up momentum by swinging, before being able to balance. Note that although a wide variety of methods can successfully learn this task given enough experience, it is a challenging domain for Bayes-adaptive algorithms, which have duly not been tried.

We use conventional parameter settings for the pendulum [5], a mass of 1kg, a length of 1m, a maximum torque of 5Nm, and coefficient of friction of 0.05 kg m^2 / s. The state of the pendulum is $s = (\theta, \dot{\theta})$. Each time-step corresponds to 0.05s, $\gamma = 0.98$, and the reward function is $\mathcal{R}(s) = \cos(\theta)$. In the initial state, the pendulum is pointing down with no velocity, $s_0 = (\pi, 0)$. Three actions are available to the agent, to apply a torque of either $\{-5, 0, 5\}$Nm. The agent does not initially know the dynamics of the pendulum. As in [5], we assume it employs independent Gaussian processes to capture the state change in each dimension for a given action. That is, $s^i_{t+1} - s^i_t \sim GP(m^i_a, \mathcal{K}^i_a)$ for each state dimension i and each action a (where $\mathcal{K}^i_a$ are Squared Exponential kernels). Since there are 2 dimensions and 3 actions, we maintain 6 Gaussian processes, and plan in the joint space of $(\theta, \dot{\theta})$ together with the possible future GP posteriors to decide which action to take at any given step.

We compare four approaches on this problem to understand the contributions of both generalization and Bayes-Adaptive planning to the performance of the agent. BAFA includes both; we also consider two non-Bayes-adaptive variants using the same simulation-based approach with value generalization. In a Thompson Sampling variant (THOMP), we only consider a single posterior sample of the dynamics at each step and greedily solve using simulation-based search. In an exploit-only variant (FA), we run a simulation-based search that optimizes a *state-only* policy over the uncertainty in the dynamics, this is achieved by running BAFA with no history feature.[4] For BAFA, FA, and THOMP, we use the same RBF network for the state-action features, consisting of 900 nodes. In addition, we also consider the BAMCP planner with an uniform discretization of the $\theta, \dot{\theta}$ space that worked best in a coarse initial search; this method performs Bayes-adaptive planning but with no value generalization.

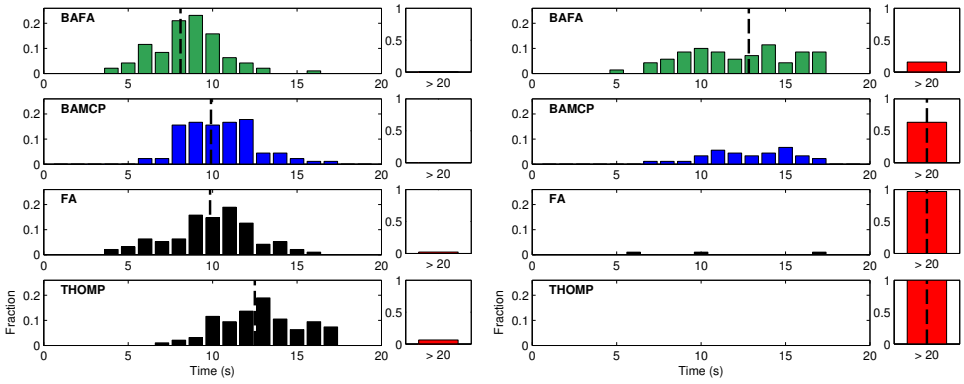

Figure 3: Histogram of delay until the agent reaches its first balance state ($|\theta| < \frac{\pi}{4}$ for $\geq$ 3s) for different methods in the pendulum domain. (a) A standard version of the pendulum problem with a cosine cost function. (b) A more difficult version of the problem with uncertain cost for balancing (see text). There is a 20s time limit, so all runs which do not achieve balancing within that time window are reported in the red bar. The histogram is computed with 100 runs with (a) $K = 10000$, or (b) $K = 15000$, simulations for each algorithm, horizon $T = 50$ and (for BAFA) $M = 50$ particles. The black dashed line represents the median of the distribution.

We allow each algorithm a maximum of 20s of interaction with the pendulum, and consider as up-state any configuration of the pendulum for which $|\theta| \leq \frac{\pi}{4}$ and we consider the pendulum balanced if it stays in an up-state for more than 3s. We report in Figure 3-a the time it takes for each method to reach for the first time a balanced state. We observe that Bayes-adaptive planning (BAFA or BAMCP) outperforms more heuristic exploration methods, with most runs balancing before 8.5s. In the Suppl. material, Figure S1 shows traces of example runs. With the same parametrization of the pendulum, Deisenroth et al. reported balancing the pole after between 15 and 60 seconds of interaction when assuming access to a restart distribution [5]. More recently, Moldovan et al. reported balancing after 12-18s of interaction using a method tailored for locally linear dynamics [15].

However, the pendulum problem also illustrates that BA planning for this particular task is not hugely advantageous compared to more myopic approaches to exploration. We speculate that this

[4]The approximate value function for FA and THOMP thus takes the form $Q(s, a) = \mathbf{w}^T \phi(s, a)$.

is due to a lack of structure in the problem and test this with a more challenging, albeit artificial, version of the pendulum problem that requires non-myopic planning over longer horizons. In this modified version, balancing the pendulum (i.e., being in the region $|\theta| < \frac{\pi}{4}$) is either rewarding ($\mathcal{R}(s) = 1$) with probability 0.5, or costly ($\mathcal{R}(s) = -1$) with probability 0.5; all other states have an associated reward of 0. This can be modeled formally by introducing another binary latent variable in the model. These latent dynamics are observed with certainty if the pendulum reaches any state where $|\theta| \geq \frac{3\pi}{4}$. The rest of the problem is the same. To approximate correctly the Bayes-optimal solution in this setting, the planning algorithm must optimize the belief-state policy *after* it simulates observing whether balancing is rewarding or not. We run this version of the problem with the same algorithms as above and report the results in Figure 3-b. This hard planning problem highlights more clearly the benefits of Bayes-adaptive planning and value generalization. Our approach manages to balance the pendulum more 80% of the time, compared to about 35% for BAMCP, while THOMP and FA fail to balance for almost all runs. In the Suppl. material, Figure S2 illustrates the influence of the number of particles M on the performance of BAFA.

5 Related Work

Simulation-based search with value function approximation has been investigated in large and also continuous MDPs, in combination with TD-learning [19] or Monte-Carlo control [3]. However, this has not been in a Bayes-adaptive setting. By contrast, existing online Bayes-Adaptive algorithms [22, 17, 1, 12, 9] rely on a tree structure to build a map from histories to value. This cannot benefit from generalization in a straightforward manner, leading to the inefficiencies demonstrated above and hindering their application to the continuous case. Continuous Bayes-Adaptive (PO)MDPs have been considered using an online Monte-Carlo algorithm [4]; however this tree-based planning algorithm expands nodes uniformly, and does not admit generalization between beliefs. This severely limits the possible depth of tree search ([4] use a depth of 3).

In the POMDP literature, a key idea to represent beliefs is to sample a finite set of (possibly approximate) *belief points* [21, 16] from the set of possible beliefs in order to obtain a small number of (belief-)states for which to backup values offline or via forward search [13]. In contrast, our sampling approach to belief representation does not restrict the number of (approximate) belief points since our belief features ($z(h)$) can take an infinite number of values, but it instead restricts their *dimension*, thus avoiding infinite-dimensional belief spaces. Wang et al.[23] also use importance sampling to compute the weights of a finite set of particles. However, they use these particles to discretize the model space and thus create an approximate, discrete POMDP. They solve this offline with no (further) generalization between beliefs, and thus no opportunity to re-adjust the belief representation based on past experience. A function approximation scheme in the context of BA planning has been considered by Duff [7], in an offline actor-critic paradigm. However, this was in a discrete setting where counts could be used as features for the belief.

6 Discussion

We have introduced a tractable approach to Bayes-adaptive planning in large or continuous state spaces. Our method is quite general, subsuming Monte Carlo tree search methods, while allowing for arbitrary generalizations over interaction histories using value function approximation. Each simulation is no longer an isolated path in an exponentially growing tree, but instead value backups can impact many non-visited beliefs and states. We proposed a particular parametric form for the action-value function based on a Monte-Carlo approximation of the belief. To reduce the computational complexity of each simulation, we adopt a root sampling method which avoids expensive belief updates during a simulation and hence poses very few restrictions on the possible form of the prior over environment dynamics.

Our experiments demonstrated that the BA solution can be effectively approximated, and that the resulting generalization can lead to substantial gains in efficiency in discrete tasks with large trees. We also showed that our approach can be used to solve continuous BA problems with non-trivial planning horizons without discretization, something which had not previously been possible. Using a widely used GP framework to model continuous system dynamics (for the case of a swing-up pendulum task), we achieved state-of the art performance.

Our general framework can be applied with more powerful methods for learning the parameters of the value function approximation, and it can also be adapted to be used with continuous actions. We expect that further gains will be possible, e.g. from the use of bootstrapping in the weight updates, alternative rollout policies, and reusing values and policies between (real) steps.

References

[1] J. Asmuth and M. Littman. Approaching Bayes-optimality using Monte-Carlo tree search. In *Proceedings of the 27th Conference on Uncertainty in Artificial Intelligence*, pages 19–26, 2011.

[2] Dimitri P Bertsekas. Approximate policy iteration: A survey and some new methods. *Journal of Control Theory and Applications*, 9(3):310–335, 2011.

[3] SRK Branavan, D. Silver, and R. Barzilay. Learning to win by reading manuals in a Monte-Carlo framework. *Journal of Artificial Intelligence Research*, 43:661–704, 2012.

[4] P. Dallaire, C. Besse, S. Ross, and B. Chaib-draa. Bayesian reinforcement learning in continuous POMDPs with Gaussian processes. In *Intelligent Robots and Systems, 2009. IROS 2009. IEEE/RSJ International Conference on*, pages 2604–2609. IEEE, 2009.

[5] Marc Peter Deisenroth, Carl Edward Rasmussen, and Jan Peters. Gaussian process dynamic programming. *Neurocomputing*, 72(7):1508–1524, 2009.

[6] MP Deisenroth and CE Rasmussen. PILCO: A model-based and data-efficient approach to policy search. In *Proceedings of the 28th International Conference on Machine Learning*, pages 465–473. International Machine Learning Society, 2011.

[7] M. Duff. Design for an optimal probe. In *Proceedings of the 20th International Conference on Machine Learning*, pages 131–138, 2003.

[8] M.O.G. Duff. *Optimal Learning: Computational Procedures For Bayes-Adaptive Markov Decision Processes*. PhD thesis, University of Massachusetts Amherst, 2002.

[9] Raphael Fonteneau, Lucian Busoniu, and Rémi Munos. Optimistic planning for belief-augmented Markov decision processes. In *IEEE International Symposium on Adaptive Dynamic Programming and reinforcement Learning (ADPRL 2013)*, 2013.

[10] J.C. Gittins, R. Weber, and K.D. Glazebrook. *Multi-armed bandit allocation indices*. Wiley Online Library, 1989.

[11] Neil J Gordon, David J Salmond, and Adrian FM Smith. Novel approach to nonlinear/non-Gaussian Bayesian state estimation. In *IEE Proceedings F (Radar and Signal Processing)*, volume 140, pages 107–113, 1993.

[12] A. Guez, D. Silver, and P. Dayan. Efficient Bayes-adaptive reinforcement learning using sample-based search. In *Advances in Neural Information Processing Systems (NIPS)*, pages 1034–1042, 2012.

[13] Hanna Kurniawati, David Hsu, and Wee Sun Lee. SARSOP: Efficient point-based POMDP planning by approximating optimally reachable belief spaces. In *Robotics: Science and Systems*, pages 65–72, 2008.

[14] H.R. Maei, C. Szepesvári, S. Bhatnagar, and R.S. Sutton. Toward off-policy learning control with function approximation. *Proc. ICML 2010*, pages 719–726, 2010.

[15] Teodor Mihai Moldovan, Michael I Jordan, and Pieter Abbeel. Dirichlet Process reinforcement learning. In *Reinforcement Learning and Decision Making Meeting*, 2013.

[16] J. Pineau, G. Gordon, and S. Thrun. Point-based value iteration: An anytime algorithm for POMDPs. In *International Joint Conference on Artificial Intelligence*, volume 18, pages 1025–1032, 2003.

[17] S. Ross and J. Pineau. Model-based bayesian reinforcement learning in large structured domains. In *Proc. 24th Conference in Uncertainty in Artificial Intelligence (UAI08)*, pages 476–483, 2008.

[18] D. Silver and J. Veness. Monte-Carlo planning in large POMDPs. In *Advances in Neural Information Processing Systems (NIPS)*, pages 2164–2172, 2010.

[19] David Silver, Richard S Sutton, and Martin Müller. Temporal-difference search in computer go. *Machine learning*, 87(2):183–219, 2012.

[20] R. S. Sutton, H. R. Maei, D. Precup, S. Bhatnagar, D. Silver, C. Szepesvári, and E. Wiewiora. Fast gradient-descent methods for temporal-difference learning with linear function approximation. In *Proceedings of the 26th Annual International Conference on Machine Learning, ICML 2009*, volume 382, page 125, 2009.

[21] Sebastian Thrun. Monte Carlo POMDPs. In *NIPS*, volume 12, pages 1064–1070, 1999.

[22] T. Wang, D. Lizotte, M. Bowling, and D. Schuurmans. Bayesian sparse sampling for on-line reward optimization. In *Proceedings of the 22nd International Conference on Machine learning*, pages 956–963, 2005.

[23] Y. Wang, K.S. Won, D. Hsu, and W.S. Lee. Monte Carlo Bayesian reinforcement learning. In *Proceedings of the 29th International Conference on Machine Learning*, 2012.

Supplementary Material

Bayes-Adaptive Simulation-based Search with Value Function Approximation

Arthur Guez, Nicolas Heess, David Silver, Peter Dayan

1 BAFA without root sampling

Algorithm 2: Bayes-Adaptive simulation-based search (no root sampling)

1: **procedure** `Search(` h_t, s_t `)`
2: **repeat**
3: `Simulate(`$h_t, s_t, 0$`)`
4: **until** `Timeout()`
5: **return** $\text{argmax}_a \; Q(h_t, s_t, a; \mathbf{w})$
6: **end procedure**
7: **procedure** `Simulate(` h, s, t `)`
8: **if** $t > T$ **then return** 0
9: $a \leftarrow \tilde{\pi}_{\epsilon-\text{greedy}}(Q(h, s, \cdot; \mathbf{w}))$
10: $s' \sim \mathcal{P}^+(h, s, a, ha\cdot, \cdot)$
11: $r \leftarrow \mathcal{R}(s, a)$
12: $R \leftarrow r + \gamma$ `Simulate(`$has', s', t+1$`)`
13: $\mathbf{w} \leftarrow \mathbf{w} - \alpha \left(Q(h, s, a; \mathbf{w}) - R\right) \nabla_{\mathbf{w}} Q(h, s, a; \mathbf{w})$
14: **return** R
15: **end procedure**

Algorithm 2 illustrates the vanilla version of online Sample-Based Planning using Monte-Carlo control without root sampling. Line 10 requires sampling from $\mathcal{P}^+$, a transition in the augmented space which integrates over the dynamics in the posterior distribution. We avoid these expensive operations at every step of the simulation with the root sampling formulation.

2 Representing the Value Function

It is known that the value function for the BAMDP is convex as a function of the belief for a particular state [1, 3] (it is piecewise linear if the horizon is finite and the state and action spaces are discrete). Suppose, for simplicity, that states and beliefs are represented exactly (i.e., for example assuming discrete states and $z_U(h) = b(h)$), then the bilinear form we introduced in Section 3.3 to represent the value function approximates the true convex value function (for a given state as a function of the belief) with a single linear function: $Q(h, s, a; \{\mathbf{w}_s\}) = \langle b(h), \mathbf{w}_s \rangle$. In general, this is not enough to represent exactly the true value function, but our experiments suggest that it is enough to reason approximately about the consequences of future beliefs.

We have also experimented with an alternative parametric form, an approximately piecewise linear form that combines multiple hyperplanes via a softmax:

$$Q(h, s, a; \{\mathbf{W}_i\}) = \sqrt[k]{\sum_i^I \left(z_U(h)^T \, \mathbf{W}_i \, \phi(s, a)\right)^k}, \tag{1}$$

inspired by the work of Parr and Russell in the contex of POMDPs [2]. The constants k and I are fixed parameters that trade-off computation and accuracy against the number of learnable parameters (the bilinear form is recovered from the soft-max form using $k = I = 1$). Given sufficient components, this form should be able to represesent the true value function arbitrarily closely. However, in our experiments with this more general form, this advantage was outweighed by its computational complexity, and it performed poorly in practice.

3 BAFA implementation details

3.1 Learning Rate Schedule

The learning rate schedule we employed for all experiment is $\alpha(n) = a_0 \frac{(n_0+1)}{(n_0+n)}$, where n is the number of weight updates, a_0 is the initial learning rate, and n_0 influences the speed of decay. We did not try to heavily optimize n_0 and a_0 for each domain, we only hand-tuned them to avoid divergence or too slow learning - we used the same values for the navigation and the pendulum task (detailed below).

3.2 Reusing Particles and Learned Weights

To avoid restarting learning from scratch at every step, we try to reuse the particles U from the previous step and warm-start weight learning from the corresponding learned values in the previous step.

To know whether the set of particles U_{t-1} can still be useful for the current planning step t (i.e., whether the particle set is not degenerate), we compute an estimate of the effective number of particles:

$$N_{\text{eff}} = \frac{1}{\sum_m z_m^{U_{t-1}}(h_t)^2}. \tag{2}$$

If $N_{\text{eff}} < \frac{M}{3}$, then we resample new particles for U_t and reinitialize the weights. Otherwise, we set $U_t = U_{t-1}$ and start learning from the previously learned $\mathbf{W}$.

4 Experimental Details

4.1 Bandit Domain

In the bandit domain, we set $a_0 = 2.5 \cdot 10^{-3}, n_0 = 2 \cdot 10^5$ for the learning rate schedule. For the exploration parameter for Monte-Carlo control, we set $\epsilon = 2 \cdot 10^{-2}$ to obtain convergence to a near-optimal policy, but different values obtain similar results and mostly affect the distance to optimality after convergence.

Note that there are not state features for this domain, and no discretization is needed for BAMCP since the observations are discrete.

4.2 Navigation Domain

The multi-scale kernel $\mathcal{K}$ is a sum of two Squared Exponential kernels ($k_\sigma(x, x') = \exp(\frac{||x-x'||^2}{2\sigma^2})$) with different length scales: $\mathcal{K}(x, x') = k_{\sigma_1}(x, x') + k_{\sigma_2}(x, x')$, where $\sigma_1 = 0.75$ and $\sigma_2 = 1.5$. In addition, some independent Gaussian observation noise is present, with zero mean and standard deviation $\sigma_n = 0.2$.

Since we cannot store exact samples from a Gaussian Process (it is infinite dimensional), we compute the posterior mean and covariance for the height according to standard formula for a set of 256 points evenly distributed in the 2-D position space. These are then used as an approximation to generate MDP dynamics for this map sample.

The state features $\phi(s)$ is a one-hot vector, obtained by binning the pose space (x, y, θ) into $D = 1024$ bins ($16 \times 16 \times 4$, uniformly for each dimension). The state-action feature vector $\phi(s, a)$ is then a vector composed of $A+1$ $D-$dimensional subvectors. Each is set to 0 except for the a-th subvector and the last subvector, which are both set to $\phi(s)$ (the last, action-independent, subvector is there to allow generalization across actions). As we also noted in the text, an RBF network can also be used here for similar results.

The discretization for BAMCP is made more efficient by only branching on a one-dimensional quantity: the observed reward z. This avoids branching on the agent's pose, something which is already approximately captured by the exact encoding of the history in BAMCP. We uniformly

segment heights with 0.5 increments between -15 and 15; this seemed to be what worked best for the number of simulations we are using in this domain.

We set $a_0 = 5 \cdot 10^{-2}, n_0 = 3 \cdot 10^5$ for the learning rate schedule. We used a more aggressive exploration rate $\epsilon = 2 \cdot 10^{-1}$ since we were more concerned about not exploring enough during search than fine-tuning a near-optimal policy.

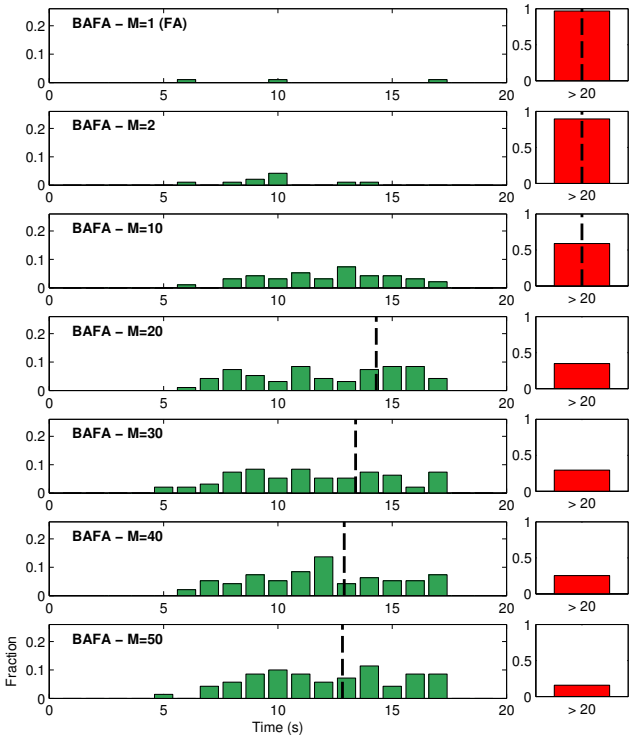

Figure S1: Histogram of delay until the agent reaches its first balance state ($|\theta| < \frac{\pi}{4}$ for ≥ 3s). The algorithm is BAFA, for different values of the number of particles in the belief representation (M), in the modified version of the pendulum problem with hidden costs. All the other parameters are as in Figure 3-b in the main text. We observe that at least around 20 particles are needed to obtain some reasonable performance in this domain. Increasing the number of particles past a certain point provides a diminishing return, since it requires more parameter to learn.

4.3 Pendulum Domain

We set the GP kernels to a Squared Exponential kernel $\mathcal{K} = l \cdot k_\sigma$, with $\sigma = 1$. In our experiments, the kernel for the velocity dimension ($\dot{\theta}$) is scaled by a factor of $l = 0.75$ and the one for the angle (θ) is scaled by a factor of $l = 0.25$. Some independent Gaussian observation noise is present, with zero mean and standard deviation $\sigma_n = 0.01$. As in all the other domains, all the compared algorithms shared the same parameters for the prior distribution.

We store the GP samples as in the navigation domain above. We also use the same parameters as above for a_0 and n_0.

The state features $\phi(s)$ (for BAFA, FA, and THOMP) is obtained from 900 Radial Basis Functions. The centers of these units are uniformly arranged in the state space. Each unit outputs a similarity measure to a $(\theta, \dot{\theta})$ vector according to:

$$\exp\left(\frac{(\pi - ||\theta - \mu_\theta| - \pi|)^2 + (\dot{\theta} - \mu_{\dot{\theta}})^2}{0.1}\right), \tag{3}$$

where $(\mu_\theta, \mu_{\dot{\theta}})$ are the unit's center coordinates. If the similarity is smaller than some small threshold, we set the corresponding entry to 0 in the feature vector in order to rely on sparse vector

computations. The state-action feature vector $\phi(s,a)$ is then obtained from $\phi(s)$ just like described in the section above.

For BAMCP, we discretized the state space uniformly into 900 bins (30×30). That was multiplied by two in the hidden cost version of the pendulum to account for the additional binary state component.

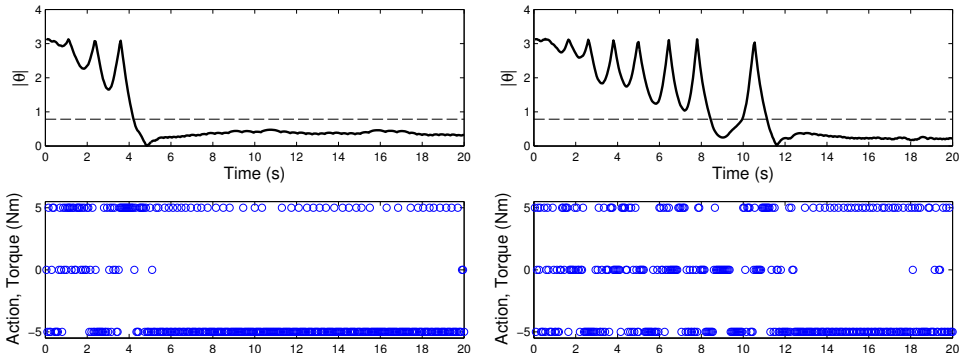

Figure S2: Two runs of BAFA on the pendulum domain, in each run this is the first few seconds of interaction of the agent with the domain. The runs are selected to illustrate a typical good run (a) and a typical slower run (b). Top row shows the absolute value of the pendulum angle θ. Bottom row shows the action selection. Dotted line marks the $\frac{\pi}{4}$ region for up-states.

References

[1] M.O.G. Duff. *Optimal Learning: Computational Procedures For Bayes-Adaptive Markov Decision Processes*. PhD thesis, University of Massachusetts Amherst, 2002.

[2] Ronald Parr and Stuart Russell. Approximating optimal policies for partially observable stochastic domains. In *IJCAI*, volume 95, pages 1088–1094. Citeseer, 1995.

[3] J.M. Porta, N. Vlassis, M.T.J. Spaan, and P. Poupart. Point-based value iteration for continuous POMDPs. *The Journal of Machine Learning Research*, 7:2329–2367, 2006.